Proton magnetic resonance spectroscopic imaging in neurodegenerative diseases

Norbert Schuff*, Peter Vermathen, Andrew A. Maudsley and Michael W. Weiner

Magnetic Resonance Unit, DVA Medical Center, and Department of Radiology, University of California, San Francisco, CA 94121, USA

Proton magnetic resonance spectroscopic imaging (^{1}H MRSI) was used to investigate changes in brain metabolites in Alzheimer's disease, epilepsy, and amyotrophic lateral sclerosis. Examples of results from several ongoing clinical studies are provided. Multislice ^{1}H MRSI of the human brain, without volume preselection offers considerable advantage over previously available techniques. Furthermore, MRI tissue segmentation and completely automated spectral curve fitting greatly facilitate quantitative data analysis. Future efforts will be devoted to obtain full volumetric brain coverage and data acquisition at short spin-echo times (TE < 30 ms) for the detection of metabolites.

MAGNETIC resonance imaging (MRI) and spectroscopy (MRS) have been used to study neurodegenerative diseases, such as Alzheimer's disease (AD) and temporal lobe epilepsy (TLE). In AD, MRI shows a general loss of cortical tissue[1] and volume reductions of the hippocampus[2,3], a region involved in declarative memory functioning. Similarly, MRI studies on TLE patients sometimes show tissue losses in the region of the seizure focus, i.e. in the hippocampus or in the neocortex[4]. Although these anatomic changes are useful for diagnosis, they are not specific for these diseases and therefore their relationship to the neurodegenerative processes remains unclear. In general, volume measurements are not a specific indicator of neuronal integrity, because volume loss may reflect a variety of mechanisms, including neuron loss, shrinkage of neuron cell bodies, or even nonneural changes such as loss of glial components. Furthermore, because pathological neuron loss is often accompanied by reactive gliosis, volume reductions may be attenuated to the extent that neurons are replaced by glia.

Proton magnetic resonance spectroscopic imaging (^{1}H MRSI) measures the regional distribution of important cerebral metabolites, although at a much coarser spatial resolution than MRI for sensitivity reasons. The most commonly observed in ^{1}H MRSI brain spectra are the resonances from the amino acid *N*-acetyl aspartate (NAA), and from choline (Cho) and creatine (Cr) containing compounds. NAA is found almost exclusively in neurons at high concentration, but is virtually undetectable in various other cell types, including glial cells[5]. NAA has therefore been described as a neuronal marker. However, diminished NAA levels cannot be unambiguously attributed to neuron loss, but may also reflect dysfunctioning of neuronal metabolism as recent ^{1}H MRSI reports of reversible NAA decrease after treatment of patients with ALS[6] or TLE[7,8] suggest. Based upon these assumptions, NAA should be a better indicator of neuron loss or dysfunction than volume measurements. NAA levels should not be spuriously increased in the presence of reactive gliosis. In fact, one would expect that gliosis, which reduces neuron density, would cause a further reduction of NAA levels. This is in contrast to volume measurements by MRI or metabolic rate measurements with positron emission tomography (PET) which reflect changes of both neuron and glia cells. Therefore, quantitative measurements of regional NAA levels by ^{1}H MRSI should be useful in the assessment of neurodegeneration.

The Cho resonance in ^{1}H MR brain spectra originates predominantly from choline itself and from glycerophosphocholine and phosphocholine, which are constituents of the membrane phospholipid metabolism[9]. Cho is known to increase markedly in conditions with myelin erosion[10], which is suspected to contribute to the pathology of AD and other diseases. Decreased NAA along with elevated Cho may therefore be useful in differentiating between axonal losses that result from myelin breakdown and those that do not. Finally, the Cr resonance represents the sum of creatine and phosphocreatine that are both present in neural and glial cells, making Cr alterations somewhat difficult to interpret.

In this report, we present recent advances from our laboratory on the application of ^{1}H MRSI in combination with MRI for the study of Alzheimer's disease, epilepsy, and amyotrophic lateral sclerosis (ALS). First, we provide a brief description of the ^{1}H MRSI methods used for these applications.

*For correspondence. (e-mail: nschuff@itsa.ucsf.edu)

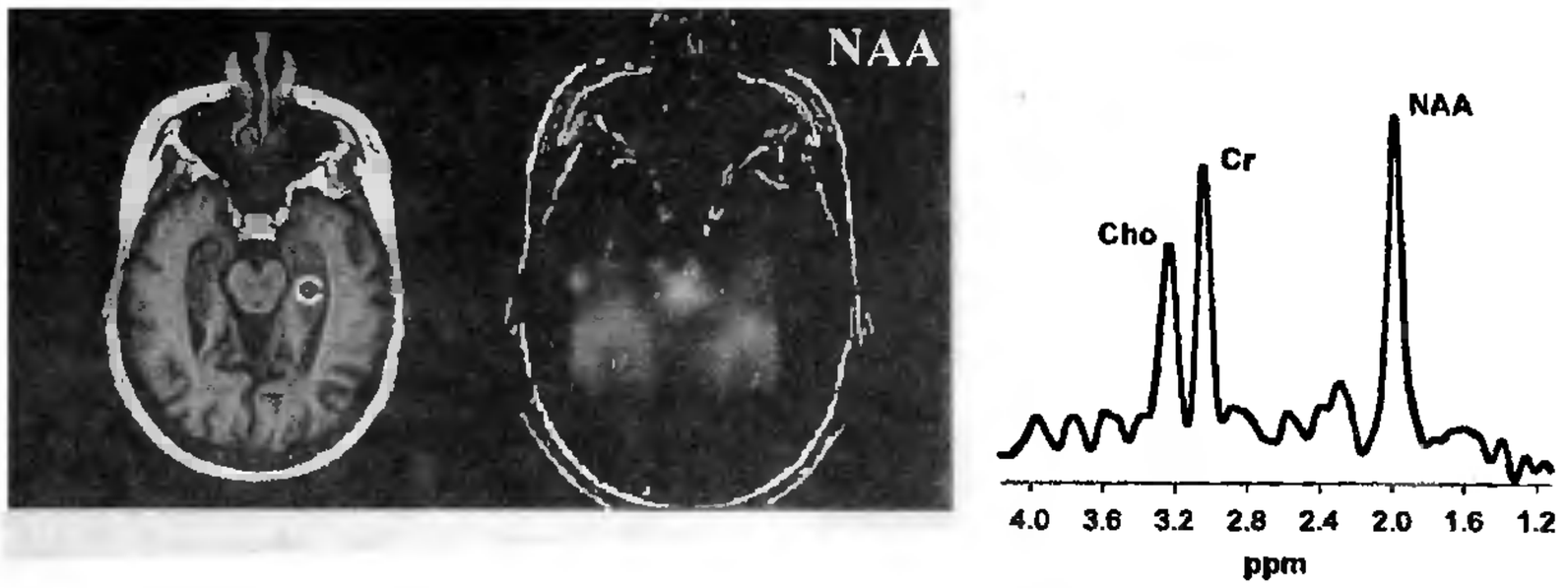

Figure 1. NAA metabolite image obtained with ^{1}H MRSI using PRESS volume preselection with coverage of the left and right hippocampus of a healthy subject. The corresponding anatomical MR image is shown on the left. The MR spectrum shown on the far right depicts the resonances from Cho, Cr, and NAA. This spectrum was selected from the body of the right hippocampus, as indicated in the anatomical MR image by the open circle.

Experimental methods

MRSI acquisition methods

MR brain studies in this laboratory and several others have predominantly been performed using the method of ^{1}H MRSI[11,12], which enables the measurement of MR metabolite spectra simultaneously from multiple areas. This is different from the more commonly reported single voxel MR spectroscopy methods, where the measurement is limited to a single region of interest at a time. This advantage of ^{1}H MRSI is of particular importance when investigating diseases that exhibit a heterogenous regional distribution of pathology, such as AD.

^{1}H MRSI combines the concept from MRI of spatial phase-encoding by stepwise increasing/decreasing magnetic field gradient pulses (after slice-selection for planar MRSI) with the acquisition of the MR signal in the presence of a highly homogeneous magnetic field to observe chemical shift metabolite spectra[11]. After Fourier transformation of the data, each of the major metabolite peaks can then be displayed as an image, coregistered to MRI[13] or other neuroimaging methods. The difficulty with ^{1}H MRSI is that low sensitivity – and the associated long acquisition time – restricts the data sampling to a limited number of phase encoding steps. The resultant truncated sampling causes poor spatial resolution due to the well-known effect of 'voxel bleeding'. This may result in a contamination of brain metabolite MR spectra with intense lipid resonances that originate from outside the brain, i.e. from the skull. One way to reduce lipid contamination is to select a spatially restricted volume prior to the ^{1}H MRSI acquisition that is sufficiently distant from the skull. A NAA metabolite image obtained with ^{1}H MRSI using volume preselection by the PRESS method[14] is shown in Figure 1, together with the corresponding MR image for better anatomical orientation. The sensitive region that is visible in the NAA metabolite image covers aspects of the mesial temporal lobe, including the left and right hippocampus. The MR spectrum shown on the far right was selected from a location in the right hippocampus and depicts the MR resonances of Cho, Cr, and NAA without interference from lipid resonances. The ^{1}H MRSI data from the hippocampus in AD and TLE presented later in this chapter were obtained by using this method.

The primary limitations of volume preselection by PRESS are that the outer cortex of the brain (an important site for many diseases) is difficult to sample and only one slice can be studied at a time. Multislice ^{1}H MRSI overcomes both the restrictions. Initially, other investigators[15] reported multislice ^{1}H MRSI that extended coverage to regions of the outer cortex, using spatially localized saturation pulses to suppress the resonances from skull lipids. However, a problem of these saturation pulses is that they may also affect metabolite resonances in the outer cortex, complicating the quantitation of metabolite concentrations in this region. To deal with the problem, our laboratory developed a multislice ^{1}H MRSI variant that avoids saturation pulses and achieves the reduction of intense lipid resonances exclusively by data post processing[16]. This is accomplished by extrapolating the measured spatial frequency distribution selectively from the signal of skull lipids to a wider range, resulting in less 'voxel bleeding' for these lipid resonances and thus, less contamination. This is demonstrated in Figure 2 *a* and *b*, where NAA metabolite images from a multislice ^{1}H MRSI acquisition are shown without and with further processing to remove all lipid signal contributions.

Spectral analysis method

For many years, metabolite MR spectra were analysed with software that required manual phasing and fitting

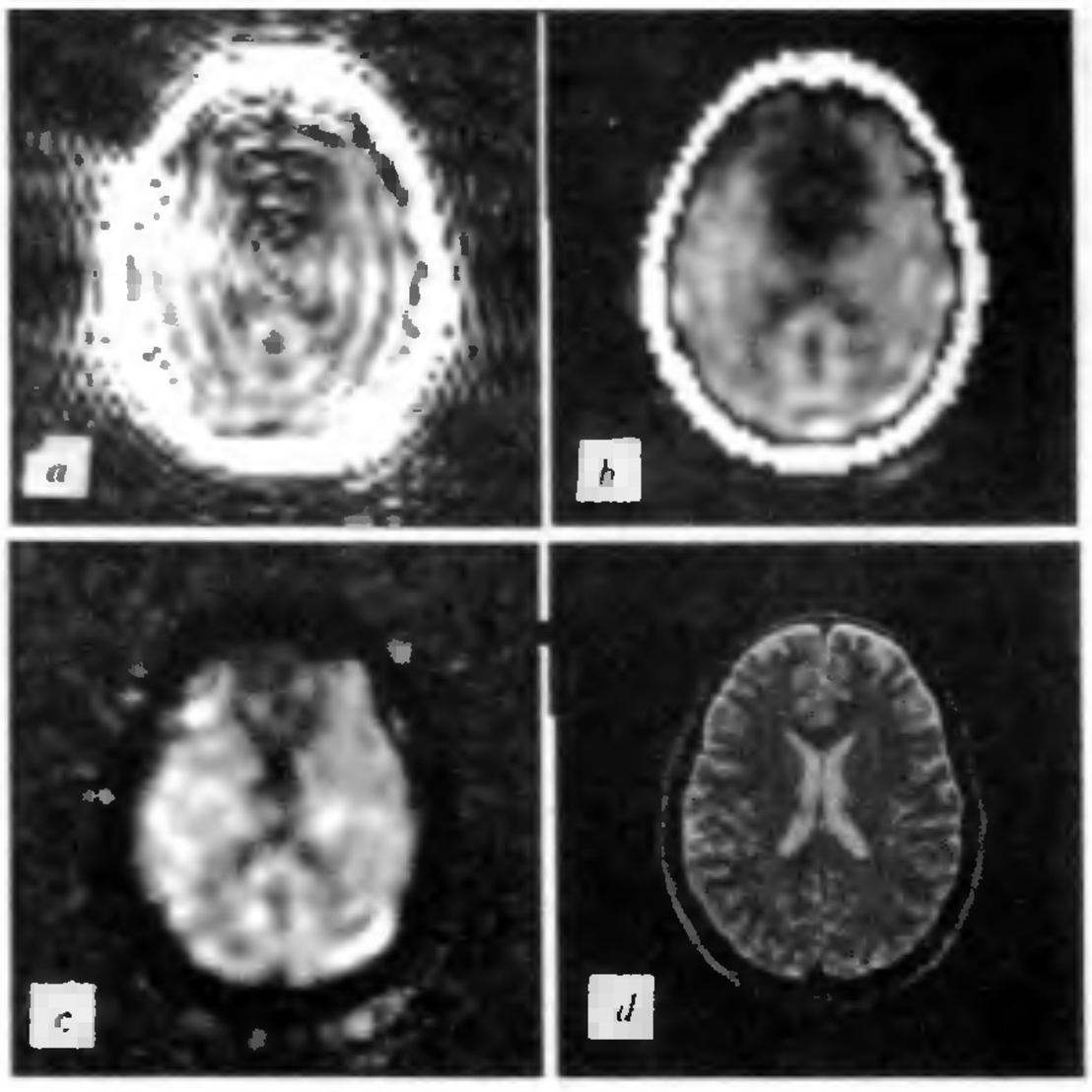

Figure 2 *a–d*. NAA images obtained using multislice ^{1}H MRSI (with a spin-echo time of 50ms) from the brain of a healthy subject. ***a***, Regular zero-filled Fourier reconstruction showing the effect of lipid contamination due to 'voxel bleeding' effects; ***b***, After frequency extrapolation of the lipid region, according to the method described in ref. 16; ***c***, After lipid extrapolation and spectral baseline correction; ***d***, Corresponding anatomical MR image.

of the resonance peaks. Besides the inefficiency of this process with respect to processing speed, another critical complication is the potential risk of operator-induced bias. Subsequently, several investigators developed algorithms that allowed an automated processing of MR spectra. Our laboratory developed a fully automated spectral fitting programme based on a parametric model that combines acquisition specific, *a priori* information with iterative wavelet-based, non-parametric characterization of baseline signals[17–19]. All *a priori* information is generated by a spectral simulation procedure[20], using the chemical shift and spin coupling parameters for each metabolite to be analysed. To form spectroscopic images, the automated spectral analysis procedure is applied to all image voxels of a MRSI data set. During the past two years we have been using these techniques in a variety of ^{1}H MRSI studies and the data presented in this chapter were processed using this approach unless otherwise noted.

MRI segmentation and co-analysis with ^{1}H MRSI data

It is well known that the variation of the brain tissue composition enclosed in a MRSI voxel can mimic changes of the metabolite peak intensities. Therefore, quantitative analysis of ^{1}H MRSI data requires that intensity changes that are due to changes of the metabolite concentration be distinguished from those that are simply artifacts of partial volume effects. This laboratory and several others have developed procedures to estimate the tissue composition of MRSI data using information from coregistered, tissue segmented MR images[21]. The calculation includes considerations of the MRSI point spread function and chemical shift displacement effects. Assume a model where, for example, contributions to the observed NAA resonance come from the grey matter (GM) and white matter (WM) with no contributions from the cerebrospinal fluid (CSF) or regions outside the brain. Then, each MRSI voxel can be characterized by two parameters, the tissue content ρ = (GM + WM) and an index for the grey matter f = GM/(GM + WM). The correction of NAA intensity for tissue volume is obtained according to $NAA^{corr} = NAA^* 1/\rho$, where NAA represents the uncorrected intensities. The index f is used in the statistical data analysis to account for variations of the GM/WM voxel composition.

Regression against tissue content and histogram analysis

Previously, investigators in this and other laboratories have analysed MRSI data by operator performed 'voxel selection' using anatomical landmarks obtained from MRI data. However, this method is subject to operator bias and between rater variability. In addition, 'voxel selection' is often complicated, because in many neurodegenerative diseases, such as AD, it is uncertain which regions are most likely to be affected in different patients. Therefore we developed new approaches that take advantage of both automated spectral fitting and automated MRI tissue segmentation which is coregistered with the MRSI. Our first approach was based on many previous reports that metabolites are different in the GM, WM and WM signal hyperintensities (WMSH). Furthermore, histopathological studies suggest that the WM and GM are affected differently in most neurodegenerative disease, e.g. AD primarily affects the GM. Therefore, we performed a regression analysis of volume corrected [NAA] as a function of the GM tissue fraction within each MRSI voxel. An extrapolation to 100% GM yields an estimate of [NAA] in 'pure' GM. Correspondingly, an extrapolation to 100% WM yields [NAA] in 'pure' WM. Our second approach was based on the hypothesis that a brain region would contain tissues at different stages of neurodegeneration and that this would be reflected by the distribution of the [NAA] concentration in the voxels across this region. This was performed using histogram analysis of atrophy corrected [NAA] values obtained from parietal lobes which con-

tained more than 70% GM (assuming that the greatest changes in AD occurred in the GM).

Experimental parameters

All studies were performed on a 1.5 T Magnetom VISION™ (Siemens Erlangen), using a standard circularly polarized head coil. T_2 and T_1-weighted MRIs were acquired for image segmentation. PRESS ^{1}H MRSI[4,9,16] was acquired using a spin-echo 2D MRSI sequence at TR/TE = 1800/135 ms with a nominal spatial inplane resolution of 9.0 × 9.0 mm^2 and a slice thickness of 15 mm. The PRESS region extended typically over 100 mm left-right and 70 mm anterior–posterior, covering both hippocampi and surrounding sections of the mesial temporal lobes. CHESS suppression pulses[22] were applied prior to the PRESS volume selection. The total acquisition time for PRESS ^{1}H MRSI was 13 min. Multislice ^{1}H MRSI data sets from three 15 mm thick slices and a nominal spatial inplane resolution of 8.0 × 8.0 mm^2 were acquired using a spin-echo sequence with TR/TE = 1800/135 ms. The total acquisition time for multislice ^{1}H MRSI was about 30 min. Along the spectral domain, data sampling was performed with a sweep width of 1000 Hz.

Initially, individual MRSI voxels were manually selected using anatomical MR images as a guide and metabolite changes were expressed as ratio values (NAA/Cr, NAA/Cho, and Cho/Cr) to eliminate partial volume effects. Subsequently for the AD and ALS studies, the spectral data were automatically processed as described above. The ^{1}H MRSI data were smoothed in the time domain using a 4Hz gaussian apodization filter and then Fourier transformed and phase- and baseline corrected. The resonance lines from NAA, Cr, and Cho were curve fitted and the values corrected for tissue volume changes, using information from the coregistered segmented MR images. Finally, the metabolite changes were expressed in mmoles/l units, using an external standard as reference.

Applications

Alzheimer's disease

Currently, it is impossible to definitively diagnose AD without brain tissue. Therefore, one goal of neuroimaging research is to develop specific and sensitive techniques for noninvasive diagnosis. Thus far, several MRI studies on AD demonstrated global cerebral atrophy[1] and specifically reduced hippocampal volumes[2]. However, a substantial overlap remains between AD patients and nondemented elderly subjects[3].

Our initial PRESS ^{1}H MRSI study of supraventricular regions in the fronto-parietal brain of AD patients showed reduced NAA levels when compared with controls[23,24]. Furthermore, these NAA reductions were independent of changes of tissue composition as measured with MRI[21], indicating that the NAA changes provided information that is not available from MRI. Subsequently, we replicated these initial findings in fronto-parietal brain on another study group[25]. In a further study on AD, we used PRESS ^{1}H MRSI to measure metabolite changes in the hippocampal region[26]. We found that atrophy corrected NAA was significantly reduced by 15.5% in the right hippocampus of AD and by 16.2% in the left hippocampus when compared with age-matched controls. The hippocampal volumes measured with MRI were also significantly reduced in AD. Importantly, the NAA and volume changes made independent contributions to the discrimination of AD from control subjects. The scatter plot of Figure 3 shows volume-corrected NAA as a function of hippocampal volume from each subject of this study. When used separately, neither hippocampal NAA nor volume could correctly classify AD patients better than 80%. When used together, however, the two measures correctly classified 90% of AD and 94% of control subjects, suggesting that hippocampal NAA measured by ^{1}H MRSI combined with measurements of hippocampal volume by MRI may improve diagnosis of AD.

In another series of yet unpublished AD studies we used multislice ^{1}H MRSI to measure metabolite changes in the outer cortex, a region which is known be affected

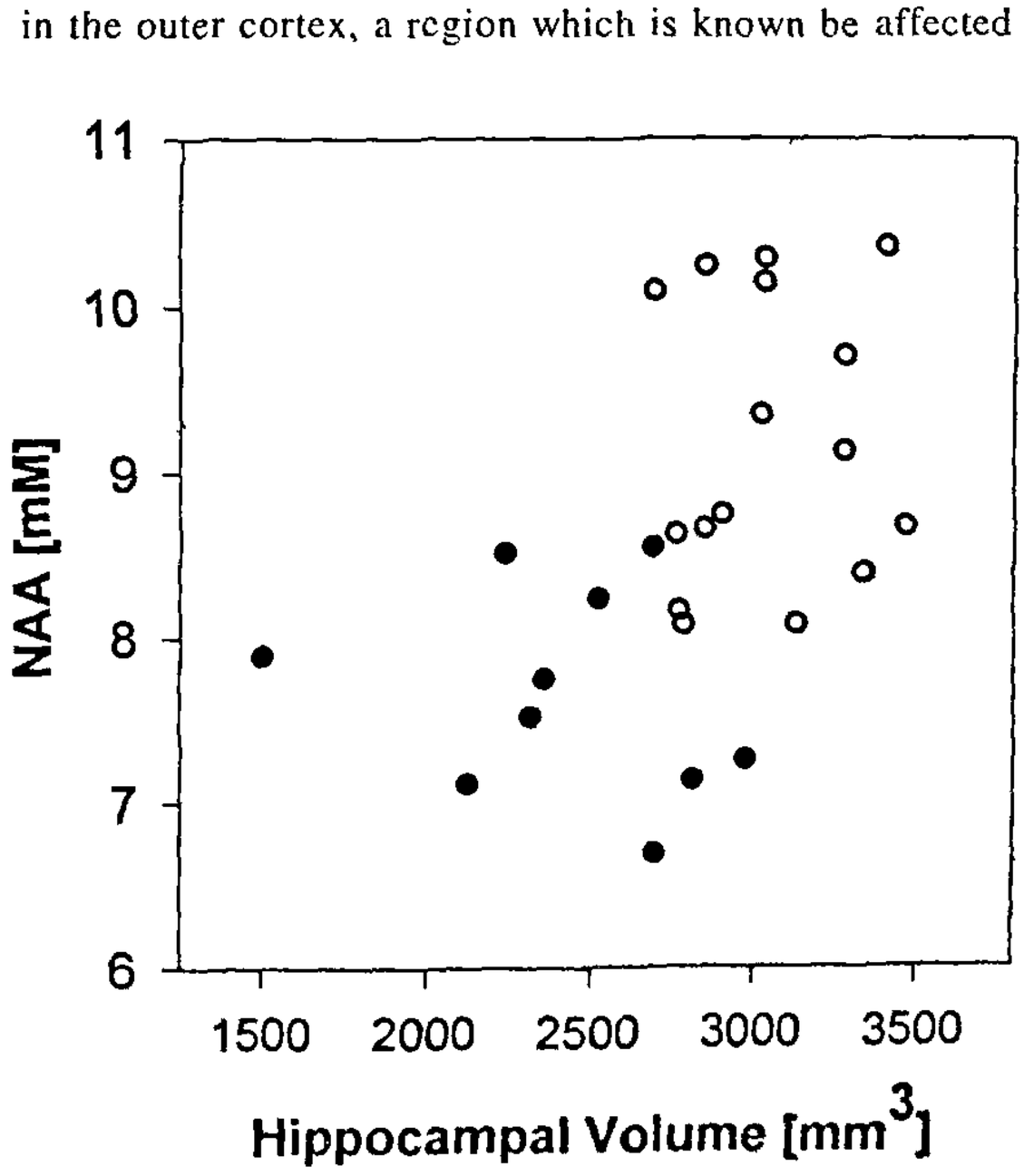

Figure 3. Atrophy corrected NAA from the hippocampus as a function of hippocampal volume from 10 AD patients (●) and 16 control subjects (○). NAA and volume are mean values of the right and left hippocampus. The unit [mM] = mmoles/l.

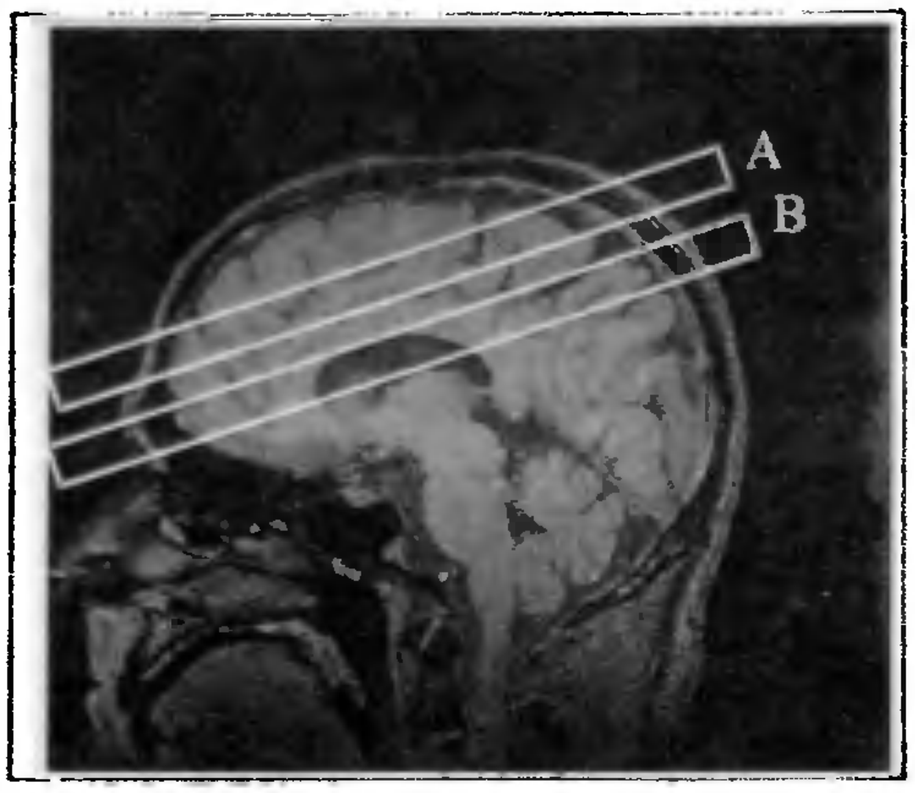

Figure 4. Slice orientation for multislice ^{1}H MRSI studies in AD. The slices cover large sections of the frontal and parietal lobes.

in AD. In Figure 4 the slice orientations used for the multislice ^{1}H MRSI studies are shown, which cover large sections of the frontal and parietal cortexes. Using regression methods to estimate the NAA concentration in the GM of the parietal and frontal cortex by extrapolation, our preliminary analysis of the data showed a 12.8% reduction of NAA levels in the parietal cortex and a 10.9% reduction in the frontal cortex of AD when compared to the controls. In contrast, the WM NAA was not significantly different. (Data from the temporal cortex have not yet been analysed using regression.) Histogram distribution of the NAA levels in parietal cortex showed that AD patients had 13.7% ($P = 0.007$) lower NAA levels compared to controls at the 50th percentile of the distribution and 16.8% ($P = 0.0005$) lower levels at the lower 10th percentile. Because these data were corrected for tissue atrophy and for variations of tissue composition, our results provide evidence that NAA reductions in AD occur independently from structural variations as measured by MRI.

Epilepsy

In TLE, it is thought that the seizure focus is localized in the hippocampus. For the surgical treatment of TLE, it is necessary to determine the location and size of the focus, and the extent to which other brain regions are affected. A variety of imaging modalities are used to evaluate TLE, including MRI, PET, and recently ^{1}H MRS. Earlier MRS studies on TLE from our laboratory[27,28] used PRESS ^{1}H MRSI to measure metabolite changes in regions of the mesial temporal lobe, including the hippocampus. Representative data from a PRESS ^{1}H MRSI study on a TLE patient are shown in Figure 5. The ^{1}H MR spectrum shown on the right was selected from the hippocampus on the side of the seizure focus (as defined by electro encephalography) and depicts a marked reduction of the NAA intensity when compared with NAA (shown in the spectrum on the left) from the other hippocampus, which has presumably not been affected by seizures. In general, our findings indicate diminished NAA levels in the ipsilateral hippocampus of TLE patients, suggesting that MRS may be useful for the lateralization of the seizure focus. Furthermore, we found that TLE patients had reduced NAA levels in the hippocampus contralateral to the seizure focus when compared with the controls. This could be due to bilateral mesial temporal sclerosis or due to repeated seizure activity. If repeated seizure activity is responsible for the reduction of NAA levels at the contralateral side, then NAA might also be reduced in other regions outside the hippocampus, suggesting metabolic change or damage to neurons.

Therefore, we tested the hypothesis that NAA is also reduced in other brain regions outside the hippocampus and the temporal lobe in TLE patients and that these NAA reductions would assist seizure focus lateralization and presurgical evaluation. For this study we used multislice ^{1}H MRSI. Representative NAA metabolite images (bottom row) of a TLE patient and the corresponding anatomical MR images (top row) are shown in Figure 6. A total of 27 voxels from 14 different regions of the brain of each subject were selected and manually processed, using the spectral analysis tools from the VISION™ system (Siemens Erlangen). We found that the NAA/(Cho + Cr) ratio of the hippocampus on the ipsilateral side of the seizure focus was significantly smaller than on the contralateral side ($P < 0.002$), confirming our previous results using PRESS ^{1}H MRSI. Furthermore, we found in many ispilateral brain regions of TLE patients smaller NAA/(Cho + Cr) values than in the corresponding brain regions of control subjects and NAA/(Cho + Cr) averaged over the ipsilateral regions in each patient was significantly smaller ($P < 0.005$) than in the controls. Finally, with the hippocampus excluded, averaged NAA/(Cho + Cr) of ipsilateral regions was still significantly lower ($P < 0.003$) in patients. This suggests that repeated seizures originating from the hippocampus may eventually lead to impairment of other brain regions. This information from multislice ^{1}H MRSI might further help the lateralization of the seizure focus.

Amyoptrophic lateral sclerosis

Amyotrophic lateral sclerosis (ALS) is a degenerative disease of both the upper and lower motor neurons, that produces progressive weakness of voluntary muscles and death in about three to five years[29]. Although a number of neuroimaging techniques have been used to study ALS, there is currently no accepted neuroimaging surrogate marker of disease activity for ALS.

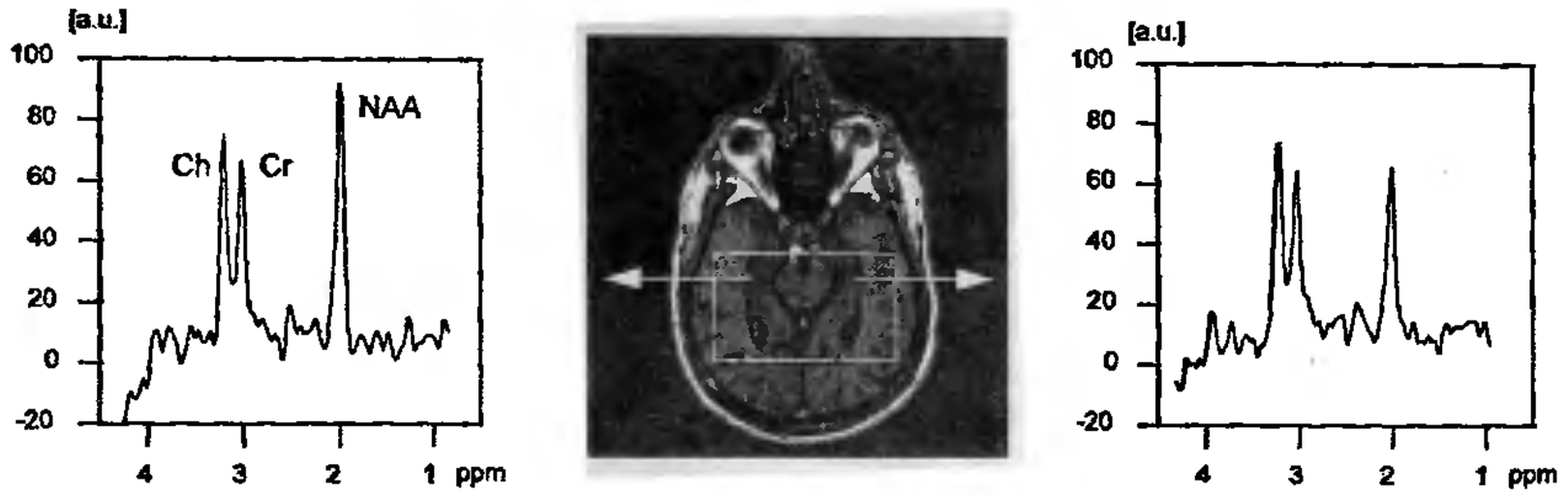

Figure 5. ^{1}H MR spectra from the left and right hippocampus of a patient with temporal lobe epilepsy. The spectrum on the right is from the hippocampus at the side of the seizure focus and reveals reduced NAA. The spectrum on the left is from the contralateral hippocampus and shows normal NAA intensity. The NAA intensity is given in arbitrary units [a.u.].

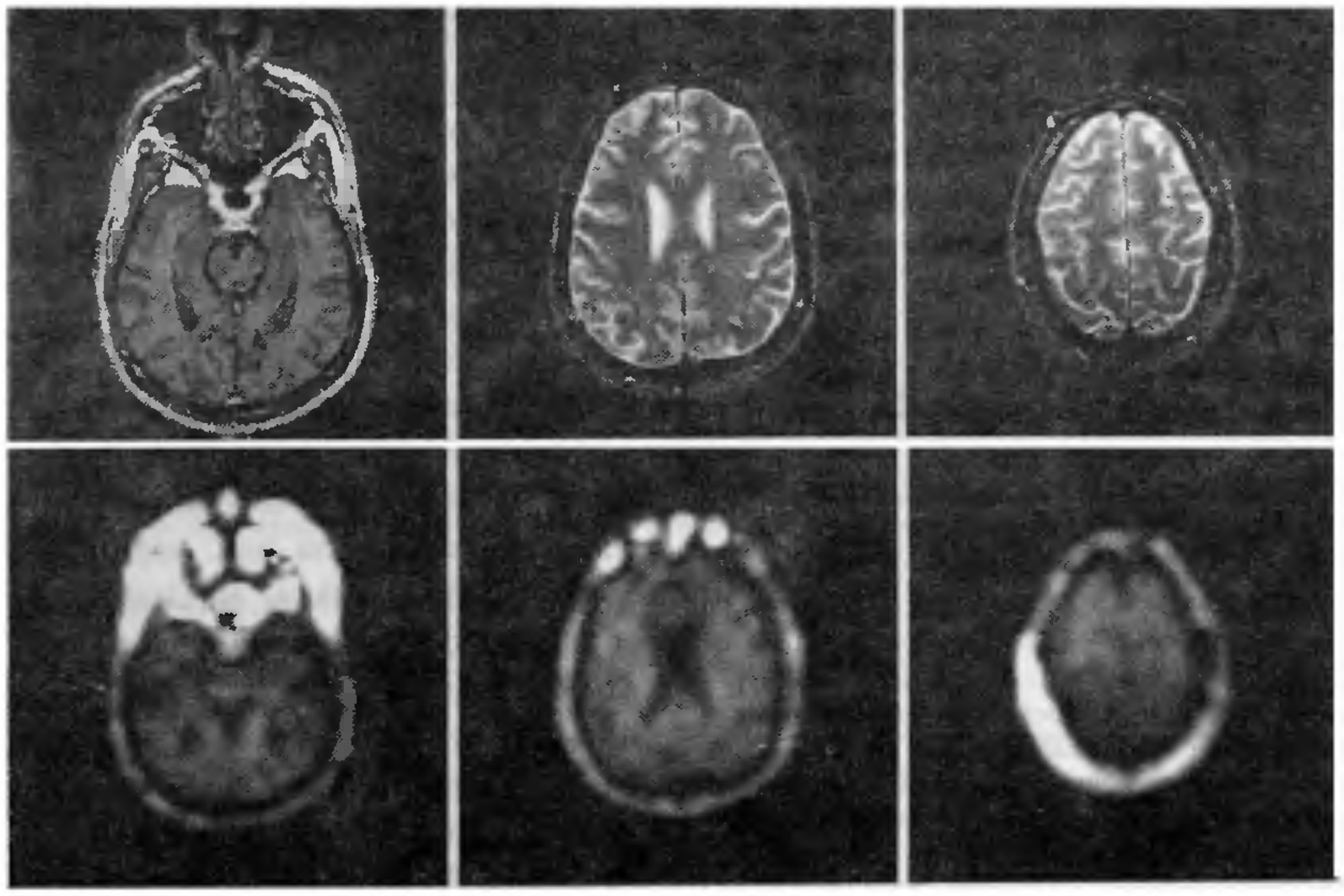

Figure 6. Representative NAA metabolite images (bottom) from a multislice ^{1}H MRSI study on a patient with temporal lobe epilepsy and the corresponding anatomical MR images (top). The orientation of the slices was selected to cover regions in the frontal, parietal, and temporal lobes, including both hippocampi.

We used multislice ^{1}H MRSI to study metabolite changes in the motor cortex and other brain regions of ALS patients. Our initial analysis of ^{1}H MRSI data from ALS patients and controls used voxel selection and measurement of metabolite changes as ratio values[30]. Table 1 lists the results, demonstrating significant decrease of NAA/(Cho + Cr) in the motor regions, but not in the non-motor regions. Subsequently, after the MRI segmentation data of the subjects were available for ^{1}H MRSI coanalysis, we quantitatively evaluated the same ^{1}H MRSI data and found that volume-corrected NAA levels remained lower in the motor cortex of ALS than in the controls. This indicates that our previous result of reduced NAA/Cr and NAA/Cho in ALS was primarily due to diminished NAA levels. Furthermore, instead of selecting only one or two regions of interest in the motor cortex, we chose all ^{1}H MRSI voxels encompassing the motor cortex and performed a histogram analysis of the NAA distributions. We expected that this approach would yield results that are less biased than results from the selection of a few regions of interest where it is often unclear whether the correct regions have been targeted. Figure 7 depicts the histogram distributions of atrophy-corrected NAA from the motor cortex in ALS and the controls, aggregated over all subjects. This clearly shows that the peak of the NAA distribution in ALS is lower than that in the controls. The mean NAA level was 28% ($P = 0.001$) lower in ALS when compared with the controls. Furthermore, the NAA distribution in ALS is bimodal with a second population of low values at about the lower 20th percentile of the distribution. At the 20th percentile, NAA levels were 30% lower

Table 1. Values of NAA/(Cho + Cr) in different brain regions of patients with ALS and controls

Group	Motor cortex	Parietal cortex	Medial GM	CS–WM	Frontal cortex	Anterior IC	Posterior IC
ALS (n = 10)	0.87 ± 0.14	0.93 ± 0.17	0.83 ± 0.10	0.81 ± 0.08	0.85 ± 0.15	0.63 ± 0.14	0.75 ± 0.15
Control (n = 9)	1.07 ± 0.11	0.99 ± 0.11	0.81 ± 0.14	0.91 ± 0.13	0.95 ± 0.17	0.74 ± 0.19	0.99 ± 0.22
%Δ	−20	−6	+3	−11	−11	−15	−24
P	< 0.005	NS	NS	< 0.06	NS	NS	< 0.05

Mean ± 1 standard deviation; NS = $P > 0.05$.
GM = grey matter; CS–WM = centrum semiovale white matter; IC = internal capsule.

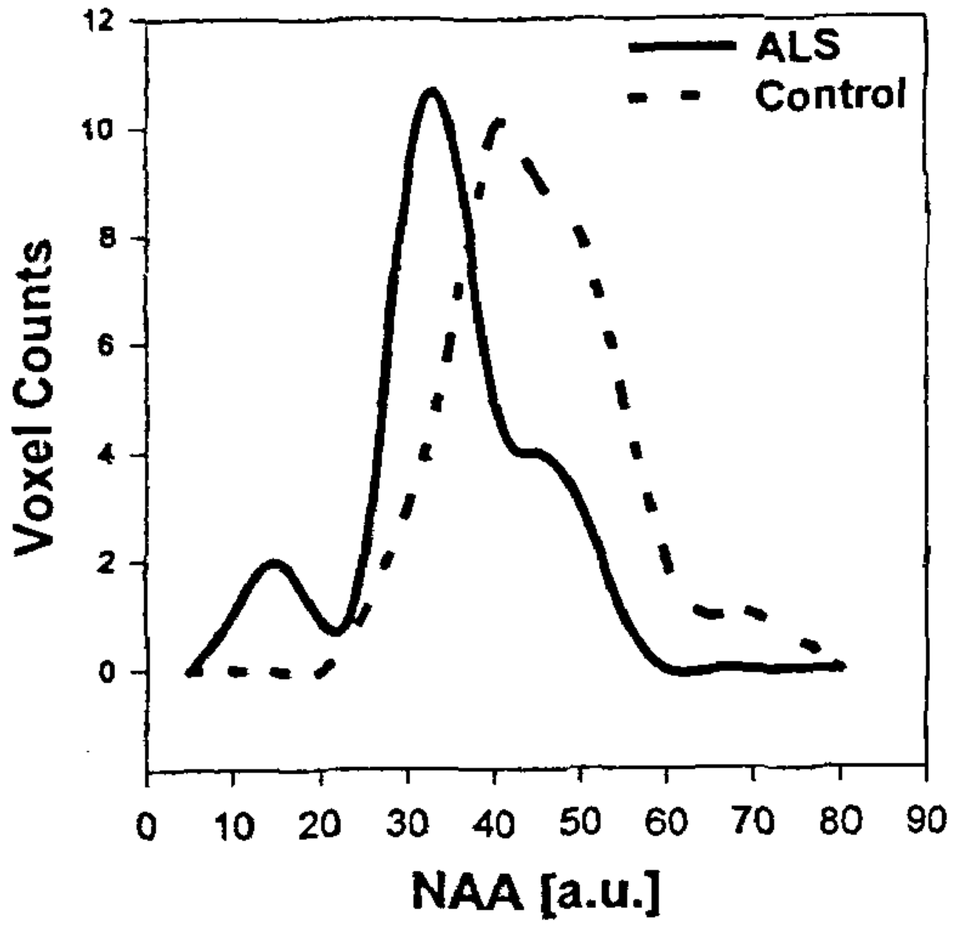

Figure 7. Histogram plots of atrophy-corrected NAA from the motor cortex in patients with amyotrophic lateral sclerosis (ALS) and the control subjects. The histograms are aggregated over 9 ALS subjects and 10 controls, respectively. The NAA intensity is given on an arbitrary scale in arbitrary units [a.u.]

in ALS than in the controls compared to a difference of 20% from our initial evaluation of NAA/(Cho + Cr) using voxel selection. The associated effect size increased from 0.9 for NAA/(Cho + Cr) to 1.8 for NAA at the lower 20th percentile, demonstrating improved discrimination of ALS from controls with histogram analysis of ^{1}H MRSI data. Whether the measurement of NAA levels in ALS with ^{1}H MRSI provides a sensitive marker for the dysfunction of upper motor neurons needs to be determined.

Limitations and conclusions

The implementation of multislice ^{1}H MRSI, without outer volume suppression pulses together with completely automated spectral fitting and co-registered MRI segmentation offers a number of advantages over previous methods. Most importantly, there is improved brain coverage, which provides greater amounts of information. Second, data analysis is almost completely automated, greatly reducing operator dependent variability. Third, metabolite changes with corrections for tissue volume and tissue composition can be evaluated quantitatively. Furthermore, this approach produces metabolite images, which ultimately may be used by clinicians for patient diagnosis.

Despite our enthusiasm for the current approach, there are a number of limitations and obvious areas for future improvement. First, ^{1}H MRSI slices are not contiguous. Another disadvantage is that multislice ^{1}H MRSI is currently obtained using rather long echo times (e.g. 135 ms). Short echo time ^{1}H MRSI is desirable to obtain information from metabolites with short T_2 such as myo-inositol and a variety of other amino acids. However, short TE ^{1}H MRSI is associated with increased lipid and water contamination and additional methods must be used to suppress these lipid and water signals. This is complicated by the fact that the magnetic field homogeneity across the brain is not uniform and shimming is difficult in the lower–anterior regions of the brain. Notwithstanding the limitations of currently available methods, data from this and other laboratories demonstrate that multislice ^{1}H MRSI is feasible, practical, and provides metabolic information about the brain that adds to information derived from MRI. As new methods are developed, and further clinical research is performed, it is expected that MRSI will be increasingly used for clinical investigation and ultimately for clinical decision making.

1. Tanabe, J. L., Amend, D., Schuff, N., DiSclafani, V., Ezekiel, F., Norman, D., Fein, G. and Weiner, M. W., *Am. J. Neurol. Res.*, 1997, **18**, 115–123.
2. Kesslak, J. P., Nalcioglu, O. and Cotman, C. W., *Neurology*, 1991, **41**, 51–54.
3. Jack, C. R., Petersen, C. R., O'Brien, P. C. and Tangalos, E. G., *Neurology*, 1992, **42**, 183–188.
4. Knowlton, R. C., Laxer, K. D., Ende, G., Hawkins, R. A., Wong, S. T., Matson, G. B., Rowley, H. A., Fein, G. and Weiner, M. W., *Ann. Neurol.*, 1997, **42**, 829–837.
5. Urenjak, J., Williams, S. R., Gadian, D. G. and Noble, M., *J. Neurochem.*, 1992, **59**, 55–61.
6. Kalra, S., Cashman, N. R., Genge, A. and Arnold, D. L., *Neurorep.*, 1998, **9**, 1757–1761.
7. Hugg, J. W., Kuzniecky, R. I., Gilliam, F. G., Morawetz, R. B., Faught, R. E. and Hetherington, H. P., *Ann. Neurol.*, 1996, **40**, 236–239.

8. Cendes, F., Andermann, F., Dubeau, F., Matthews, P. M. and Arnold, D. L., *Neurology*, 1997, **49**, 1525–1533.
9. Barker, P. B., Breiter, S. N., Soher, B. J., Chatham, J. C., Forder, J. R., Samphilipo, M. A., Magee, C. A. and Anderson, J. H., *Magn. Reson. Med.*, 1994, **32**, 157–163.
10. Chang, L., Ernst, T., Tornatore, C., Aronow, H., Melchor, R., Walot, I., Singer, E. and Cornford, M., *Neurology*, 1997, **48**, 836–845.
11. Maudsley, A. A., Hilal, S. K., Perman, W. H. and Simon, H. E., *J. Magn. Reson.*, 1983, **51**, 147–152.
12. Brown, T. R., Kincaid, B. M. and Ugurbil, K., *Proc. Natl. Acad. Sci. USA*, 1982, **79**, 3523–3526.
13. Maudsley, A. A., Matson, G. B., Hugg, J. W. and Weiner, M. W., *Int. Soc. Opt. Eng.*, 1993, **1887**, 282–289.
14. Bottomley, P. A., *Selective Volume Method for Performing Localized NMR Spectroscopy*, US patent 4 480 228, 1984.
15. Duyn, J. H., Gillen, J., Sobering, G., van Zijl, P. C. and Moonen, C. T., *Radiology*, 1993, **188**, 277–282.
16. Haupt, C. I., Schuff, N., Weiner, M. W. and Maudsley, A. A., *Magn. Reson. Med.*, 1996, **35**, 678–687.
17. Young, K., Govindaraju, V., Soher, B. J. and Maudsley A. A., *Magn. Reson. Med.*, 1998, **40**, 812–815.
18. Young, K., Soher, B. J. and Maudsley, A. A., *Magn. Reson. Med.*, 1998, **40**, 816–821.
19. Soher, B. J., Young, K., Govindaraju, V. and Maudsley, A. A., *Magn. Reson. Med.*, 1998, **40**, 822–831.
20. Smith, S. A., Levante, T. O., Meier, B. H. and Ernst, R. R., *J. Magn. Reson.*, 1994, **A106**, 75–105.
21. MacKay, S., Ezekiel, F., Di Sclafani, V., Meyerhoff, D. J., Gerson, J., Norman, D., Fein, G. and Weiner, M. W., *Radiology*, 1996, **198**, 537–545.
22. Haase, A., Frahm, J., Hänicke, W. and Matthaei, D., *Phys. Med Biol.*, 1985, **30**, 341–344.
23. Meyerhoff, D. J., MacKay, S., Constans, J. M., Norman, D., Van Dyke, C., Fein, G. and Weiner, M. W., *Ann. Neurol.*, 1994, **36**, 40–47.
24. MacKay, S., Meyerhoff, D. J., Constans, J. M., Norman, D., Fein, G. and Weiner, M. W., *Arch. Neurol.*, 1996, **53**, 167–174.
25. Schuff, N., Amend, D. L., Meyerhoff, D. J., Tanabe, J. L., Norman, D., Fein, G. and Weiner, M. W., *Radiology*, 1998, **207**, 91–102.
26. Schuff, N., Amend, D., Ezekiel, F., Steinman, S. K., Tanabe, J., Norman, D., Jagust, W., Kramer, J. H., Mastrianni, J. A., Fein, G. and Weiner, M. W., *Neurology*, 1997, **49**, 1513–1521.
27. Ende, G. R., Laxer, K. D., Knowlton, R. C., Matson, G. B., Schuff, N., Fein, G. and Weiner, M. W., *Radiology*, 1997, **202**, 809–817.
28. Vermathen, P., Ende, G., Laxer, K. D., Knowlton, R. C., Matson, G. B. and Weiner, M. W., *Ann. Neurol.*, 1997, **42**, 194–199.
29. Ringel, S. P., Murphy, J. R., Alderson, M. K., Bryan, W., England, J. D., Miller, R. G., Petajan, J. H., Smith, S. A., Roelofs, R. I. and Ziter, F., *Neurology*, 1993, **43**, 1316–1322.
30. Rooney, W. D., Miller, R. G., Gelinas, D., Schuff, N., Maudsley, A. A. and Weiner, M. W., *Neurology*, 1998, **50**, 1800–1805.

ACKNOWLEDGEMENTS. We thank Drs William Jagust, Mort Lieberman, and Owen Wolkowitz for referring AD patients, Drs Robert Miller and Deborah Gelinus for referring ALS patients and Dr William Rooney for providing the MR data from these patients, Drs Karl Young and Brian Soher for development and assistance of the automated spectral analysis, Dr Kenneth Laxer for referring epilepsy patients and Dr Gabriel Ende for performance of some epilepsy experiments, Dr Diane Amend for segmentation of MRI data, and Mr Frank Ezekiel for implementation of the MRI segmentation and coregistration software. Financial support was provided in part by the VA Medical Research Service and NIH grants AG 10897 and AG12119.